Primordial Carbonylated Iron-Sulfur Compounds and the Synthesis of Pyruvate

George D. Cody *et al.*

Science **289**, 1337 (2000);
DOI: 10.1126/science.289.5483.1337

22. M. Chaussidon and F. Robert, *Earth Planet. Sci. Lett.* **164**, 577 (1998).
23. M. Zhai, E. Nakamura, D. M. Shaw, T. Nakano, *Geochim. Cosmochim. Acta* **60**, 4877 (1996).
24. Although Be is concentrated in melilite, large Be/B fractionations are achieved only when the degree of B depletion is also high. In the case of Allende 3529-30, B abundances are not depleted but are instead enriched relative to CI values. One analyzed spot, with a B concentration of ~10 ppm, consists primarily of fine-grained alkali-rich minerals thought to be secondary phases produced during alteration of the original CAI assemblage. We interpret the high B abundances and near-normal δ^{11}B values of 3529-30 as reflecting the reintroduction of B into the CAI during the secondary alteration event(s), whether in the nebula or in an asteroidal setting. Recent ion microprobe measurements [K. K. Marhas and J. N. Goswami, *Curr. Sci.* **78**, 78 (2000)] of B in anorthite from an Efremovka CAI show normal δ^{11}B values, consistent with the high B concentrations and low Be/B expected for anorthite.
25. E. D. Feigelson and T. Montmerle, *Annu. Rev. Astron. Astrophys.* **37**, 363 (1999).
26. N. Prantzos, M. Cassé, E. Vangioni-Flam, in *Origin and Evolution of the Elements*, N. Prantzos, E. Vangioni-Flam, M. Cassé, Eds. (Cambridge Univ. Press, Cambridge, 1993), pp. 156–167.
27. A. Lukasiak, P. Ferrando, F. B. McDonald, W. R. Webber, *Astrophys. J.* **423**, 426 (1994).
28. D. D. Clayton and L. Jin, *Astrophys. J.* **451**, 681 (1995).
29. A. G. W. Cameron, P. Hoflich, P. C. Myers, D. D. Clayton, *Astrophys. J.* **447**, L53 (1995).
30. R. I. Epstein, *Astrophys. J.* **212**, 595 (1977).
31. H. Bloemen *et al.*, *Astrophys. J. Lett.* **521**, L137 (1999).
32. J. Igea and A. E. Glassgold, *Astrophys. J.* **518**, 848 (1999).
33. T. Montmerle, in *Astronomy with Radioactivities*, R. Dehl and D. Hartmann, Eds. (MPE Report 274, Max-Planck-Institut für Extraterrestriche Physik, Garching, Germany, 1999), pp. 225–236.
34. The X-wind model makes definitive predictions for irradiation of CAI precursors based on a scaling of x-ray luminosity of YSOs to the flux of particles accelerated in solar flares (*5*). With cross sections for ^{16}O(p,x)^{10}Be from (*13*) and assuming an energy spectrum characteristic of impulsive flares that scales as $E^{-3.5}$, and estimating the ^{9}Be concentration in the CAI 3529-41 as ~350 ppb (~14 × CI), we calculate [equation 20 of (*5*)] an initial ^{10}Be/^{9}Be of 0.0005, which is within a factor of 2 of the measured value. A deficit of this magnitude is within the systematic uncertainties of these calculations and can be made up by either a slightly flatter proton spectrum or a substantial contribution to ^{10}Be production from He spallation. The same irradiation parameters and cross sections summarized in (*9*) yield values of ^{41}Ca/^{40}Ca and ^{53}Mn/^{55}Mn that are compatible with those observed in CAIs (*5*).
35. G. J. MacPherson, A. M. Davis, E. K. Zinner, *Meteoritics* **30**, 365 (1995).
36. S. B. Simon, L. Grossman, A. M. Davis, *Geochim. Cosmochim. Acta* **55**, 2635 (1991).
37. M. Chaussidon, F. Robert, D. Mangin, P. Hanon, E. F. Rose, *Geostandards Newsl.* **21**, 7 (1997).
38. Work made possible by grants from INSU-CNRS-PNP and NSF International Programs/Instrumentation and Facilities. Additional support from NASA.

28 March 2000; accepted 19 July 2000

Primordial Carbonylated Iron-Sulfur Compounds and the Synthesis of Pyruvate

George D. Cody,* Nabil Z. Boctor, Timothy R. Filley, Robert M. Hazen, James H. Scott, Anurag Sharma, Hatten S. Yoder Jr.

Experiments exploring the potential catalytic role of iron sulfide at 250°C and elevated pressures (50, 100, and 200 megapascals) revealed a facile, pressure-enhanced synthesis of organometallic phases formed through the reaction of alkyl thiols and carbon monoxide with iron sulfide. A suite of organometallic compounds were characterized with ultraviolet-visible and Raman spectroscopy. The natural synthesis of such compounds is anticipated in present-day and ancient environments wherever reduced hydrothermal fluids pass through iron sulfide–containing crust. Here, pyruvic acid was synthesized in the presence of such organometallic phases. These compounds could have provided the prebiotic Earth with critical biochemical functionality.

In all extant organisms, transition metal sulfide clusters play a crucial catalytic role in biological energy conversion systems (*1*). The potential connection between this essential role and the predominance of mineral sulfides in hydrothermal and volcanic vents has led some to speculate that life may have emerged from such environments (*2*). Such a connection is further supported by the natural history of bacterial lineages (*3*).

Recently, experiments designed to replicate aspects of the primitive hydrothermal vent solution chemistry have revealed the intrinsic potential for the synthesis of alkyl thiols (*4*) from reactions involving iron sulfides in the presence of CO. The formation of acetate (*5*) has been demonstrated in aqueous solutions containing methyl thiol and CO in the presence of iron and nickel sulfides. Huber and Wächtershäuser (*5*) proposed that iron and nickel sulfides grossly mimic the functionality of acetyl coenzyme A (CoA) synthase, the iron- and nickel-containing enzyme complex present in chemoautotrophic anaerobic organisms (*6*).

In the experiments described above, surfaces of transition metal sulfides presumably served to bind both alkyl groups and carbon monoxide, thus promoting carbon reduction as well as carbonyl insertion reactions (*7*). Both these experiments were performed at relatively low temperatures and pressures. At elevated temperatures and pressures, such as those attained in shallow oceanic crust, transition metal sulfides are likely to react with both CO and alkyl thiols (and/or disulfides) to produce sulfur-containing transition metal carbonyls (*8*). The natural synthesis of such compounds through the interaction of reduced crustal fluids with transition metal sulfides precipitated in Hadean crust could have provided a natural source for carbonylated organometallic species. Here, we describe the results of geochemical experiments that explore the formation of such complexes under conditions of high pressure and temperature.

Our experiments were run in welded gold tube reactors charged with 15.0 mg (170 μmol) of pure iron sulfide (*9*), 5.0 mg (31 μmol) of alkyl (nonyl) thiol, and 5.0 mg (110 μmol) of formic acid (99.9%). Formic acid was used as a source of reactive C_1 (organic molecules with one C atom); that is, CO and H_2O are formed through the thermal decomposition of formic acid (*10*) and equilibrated with CO_2 and H_2 through the water-gas shift reaction. Although formic acid was chosen primarily as a source of CO, it has been detected in present-day vent fluids (*11*). The initial concentrations of thiol and C_1 compounds were chosen to ensure a large excess of substrate per available mineral surface area [~10,000 substrate molecules per surface site (*12*)]. Multiple experiments were run at elevated pressures (50, 100, and 200 MPa) and held at 250° ± 0.2°C for 6 hours with the use of a gas pressure apparatus (*13*). Additional blank experiments in Au (without minerals) were run and analyzed under identical conditions to address the potential catalytic activity of Au; the results revealed only nonyl thiol as the recovered product.

After reaction, each reactor was stored frozen at −87°C until processing and was immersed in liquid N_2 immediately before opening. Quantitative analysis of nonyl-containing organic compounds was performed on triplicate runs obtained at each pressure, with the use of gas chromatography–mass spectrometry (GC-MS) detection, a calibration standard, and standard esterification proce-

Geophysical Laboratory, Carnegie Institution of Washington, 5251 Broad Branch Road, NW, Washington, DC 20015, USA.

*To whom correspondence should be addressed.

dures (*14*). Aqueous extracts were analyzed with both high-performance liquid chromatography (HPLC) and GC-MS (*15*). Ultraviolet (UV)-visible spectra were acquired on duplicate-run product solutions diluted in 1 ml of acetonitrile. Raman spectra were acquired on undiluted solutions transferred into quartz tubes (*16*).

The synthesis of 1-decanoic acid (Fig. 1) reveals that carbonylation occurred under these conditions. Formation of 1-methylnonyl sulfide and 1-(methylthio)-1-(nonylthio)-nonane (Fig. 1) reveals that a portion of CO was reduced to methyl groups. Other major products included dinonyl sulfide, disulfide, and trisulfide. With increasing pressure, the total recovery of nonyl-containing compounds decreased substantially.

A probable sink for the nonyl-containing products under these reaction conditions is the formation of nonyl-containing organometallic phases (*8*). The product liquids recovered from the reactors were clear but colored, grading from pale yellow (at 50 MPa) up to a deep orange-red (at 200 MPa). In reaction mixtures containing only formic acid and FeS (250°C, 200 MPa, 6 hours), the solution appeared colorless. The UV-visible spectrum (Fig. 2A), however, revealed a modest amount (3.7 μmol) of iron pentacarbonyl, corresponding to ~2.0% of the iron initially present as sulfide and 17% of the available C_1 bound as CO.

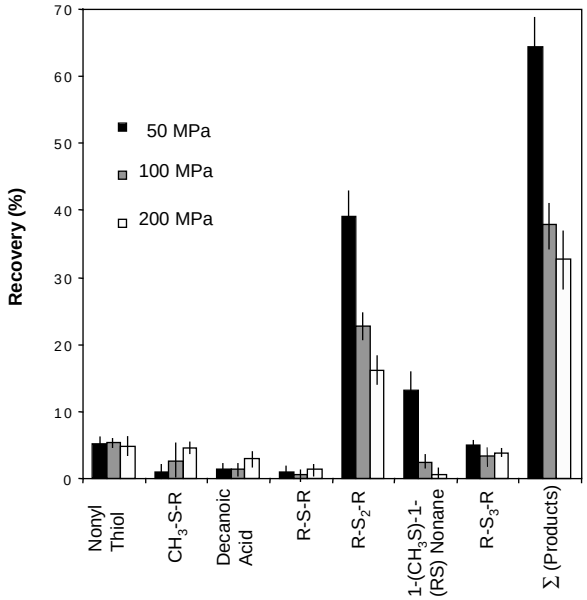

Fig. 1. Average product distribution ($n = 3$) for reactions of nonyl thiol and formic acid in the presence of FeS at 250°C and at pressures of 50, 100, and 200 MPa (R = nonyl group). Product yield is expressed as the percentage of recovered compounds with respect to the initial amount of nonyl thiol (in moles). Error bars show statistical variation (2σ).

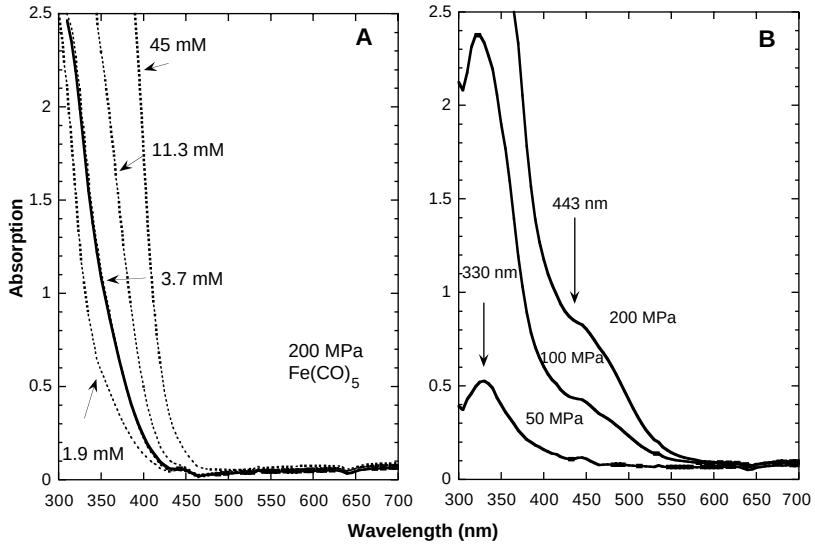

Fig. 2. (**A**) UV-visible spectrum of the product solution (diluted in 1 ml of acetonitrile) derived from reaction of formic acid in the presence of FeS at 250°C and 200 MPa for 6 hours. The solid line is the reaction solution; the dashed lines are calibration curves derived from known concentrations of $Fe(CO)_5$. (**B**) UV-visible spectra of product solutions (in 1 ml of acetonitrile) derived from the reaction of nonyl thiol and formic acid in the presence of FeS at 250°C and 50, 100, or 200 MPa for 6 hours.

The UV-visible spectra of runs containing nonyl thiol exhibit significantly different absorption spectra, with a peak at ~330 nm and a distinct shoulder at ~443 nm (Fig. 2B). Raman spectroscopy revealed a continuum of CO stretching vibrations from 1905 to 2090 cm^{-1}, with peaks at 1930, 1984, 2040, and 2073 cm^{-1}. Given the relatively extreme experimental conditions, it is probable that a number of carbonylated and nonylated iron-sulfur compounds contribute to these spectra. One carbonylated species particularly likely to be present in the product suite is the organometallic compound $Fe_2(RS)_2(CO)_6$ [where R = nonyl (*8*)]. The reported UV-visible spectrum of the two-iron cluster $Fe_2(CH_3S)_2(CO)_6$ is similar to that shown in Fig. 2A (*17*). Reaction of $Fe(CO)_5$ with dimethyldisulfide at elevated CO pressures has been shown to result in high yields of $Fe_2(CH_3S)_2(CO)_6$ (*8, 17*). The results of the present experiments suggest a generalized reaction whereby iron sulfide is consumed to produce a carbonylated iron-sulfur cluster and excess sulfur, for example,

$$2FeS + 6CO + 2RSH \rightarrow$$

$$Fe_2(RS)_2(CO)_6 + 2S^0 + H_2 \qquad (1)$$

Production of excess S^0 was confirmed by the formation of dinonyl trisulfide (Fig. 1). Analysis of the residual mineral phase reveals no significant change in stoichiometry, indicating congruent dissolution of FeS (*18*). The Raman data, however, indicate that other organometallic species are clearly present, and Eq. 1 is just one of many likely reactions. The synthesis of carbonylated iron-containing species was enhanced with pressure (Fig. 2B); the intensity of the 330- and 454-nm bands in the UV-visible spectra increased by a factor of ~13 as the pressure was increased from 50 to 200 MPa.

In their low-temperature, low-pressure study, Huber and Wächtershäuser (*5*) reported that FeS exhibited no catalytic effect for the promotion of carbonyl insertion. The presence of significant quantities of carbonylated iron-sulfur clusters in the reaction products described above suggests that it may be these compounds, not the mineral surfaces, that promoted the carbonylation reactions observed in our experiments.

The facile synthesis of significant quantities of carbonylated iron-sulfur clusters in the present experiments suggests that in natural settings, where reduced hydrothermal fluids pass through sulfide-containing crust, significant concentrations of these potentially catalytic species will form. Provided that the CO pressure remains high enough, transport of iron and sulfur to low-

er temperature environments within a ridge system is probable. Formic acid and CO are observed in some present-day vent fluids (*11, 19*); given a more reduced mantle in Hadean times, there may have been considerably more CO available for the synthesis of carbonylated transition metal clusters. Such a possibility indicates that if Earth's first life arose in the flank regions of oceanic spreading centers, it would have had a ready source of both reduced carbon and iron to facilitate primary metabolism.

The presence of such complexes may have provided important functionality in the earliest stages of life. For example, the conversion of $Fe_2S_2(CO)_6$ to produce the two-center ferredoxin-like complex anion $Fe_2(RS)_4S_2^{-2}$ has been reported (*20*); the promotion of such chemistry in a prebiotic world could yield ferredoxin-like cofactors essential for electron transport. Partial retention of some carbonylated character might have served other critical functions. For example, Peters *et al*. (*21*) recently showed that the active center of the hydrogenase enzyme isolated from *Clostridium pasteurianum* contains a two-iron cluster that is either carbonylated or cyanated (or both).

The function of this center appears to be the generation of H_2 by reduction of H^+ using electrons transported along a chain of Fe_4S_4 clusters from the enzymatic site of pyruvate oxidation (*22, 23*). Because the activity of H_2 is high in the present experiments, it is possible that under these conditions $Fe_2(RS)_2(CO)_6$—and/or other organometallic phases containing iron and sulfur—might operate in the opposite sense and promote the synthesis of α-keto acids in addition to the observed singly carbonylated products such as decanoic acid (Fig. 1). Analysis of the derivatized products with GC-MS did not reveal unambiguous evidence for the formation of 2-oxo-undecanoic acid. Pyruvic acid was detected (*23*), however, with a yield of 0.07% of the initial C_1 obtained at 200 MPa. Using selective ion monitoring to enhance sensitivity, we measured an increased yield of pyruvic acid with pressure (Fig. 3). The actual yield of pyruvic acid must be larger than 0.07% because the available C_1 must be less than the initial amount of C_1, as judged by the extensive formation of carbonylated iron-sulfur clusters.

The synthesis of pyruvic acid from the intrinsic constituents of an iron-, sulfur-, and CO-rich environment is a critical step for the origin of life, as many extant biosynthetic pathways branch from pyruvate. Huber and Wächtershäuser demonstrated that transition metal sulfides can initiate the fixation of carbon through a mechanism that mimics the synthesis of acetyl CoA (*5*). Entry into primitive anaerobic metabolism, however, requires the next step, the synthesis of pyruvic acid.

From the perspective of an ideal environment suitable for the emergence of life, a promising hypothesis would have the synthesis of carbonylated iron-sulfur catalysts occurring at higher temperatures and pressures (e.g., 200° to 300°C and 100 to 200 MPa), followed by advection of such compounds to lower temperature regimes (e.g., 90° to 150°C). Lower temperatures found nearer to the crust-ocean interface may be more conducive to the survivability of important biomolecules such as α-keto acids. These results lend support to the theory that the shallow Hadean oceanic crust could have provided Earth's most primitive life with a warm enclave continuously flooded by fluids rich in reduced carbon, electron acceptors such as S^0, and potentially catalytic carbonylated iron-sulfur clusters.

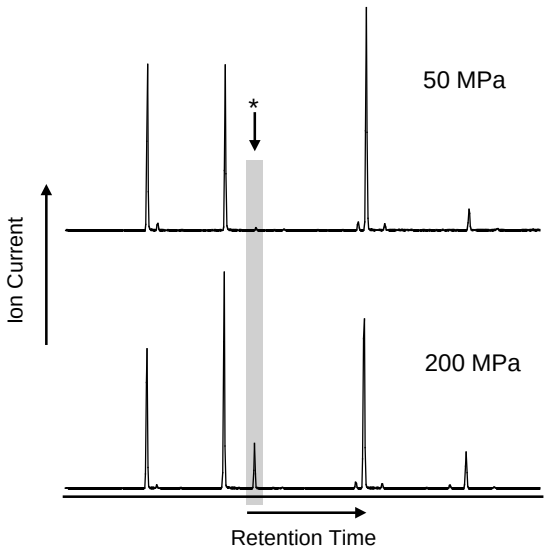

Fig. 3. Chromatograms for runs of nonyl thiol and formic acid in the presence of FeS at 250°C for 6 hours at 50 or 200 MPa. The presence of the pyruvate ester (highlighted in the gray box) is amplified with selective monitoring of ions with charge/mass ratio (*m*/*z*) values of 61, 89, 103, 131, and 145, characteristic of the pyruvate derivative, to enhance the detection limits. Analysis of underivatized aqueous extracts with both HPLC and GC-MS also revealed the presence of acetic acid, methyl thiol, and H_2S. Formation of methyl thiol in the presence of FeS and CO has been demonstrated (*4*) and is required on the synthesis path toward pyruvic acid. Acetate was present in low abundance (~0.05% the amount of initial C_1) and is anticipated both as a hydrolytic intermediate in the synthesis of pyruvate and as a thermal decomposition product of pyruvate at high temperatures.

References and Notes

1. T. G. Spiro, Ed., *Iron-Sulfur Proteins* (Wiley, New York, 1982); H. Beinert, R. H. Holm, E. Münck, *Science* **277**, 653 (1997).
2. G. Wächtershäuser, *Prog. Biophys. Mol. Biol.* **58**, 85 (1992); R. Cammack, in *Origin and Evolution of Biological Energy Conversion*, H. Baltscheffsky, Ed. (VCH, New York, 1996), pp. 43–69.
3. N. R. Pace *et al*., *Proc. Natl. Acad. Sci. U.S.A.* **93**, 9188 (1996); N. R. Pace, *Science* **276**, 734 (1997).
4. W. Heinen and A. M. Lauers, *Orig. Life Evol. Biosphere* **26**, 131 (1996).
5. C. Huber and G. Wächtershäuser, *Science* **276**, 245 (1997).
6. D. Qiu, M. Kumar, S. W. Ragsdale, T. G. Spiro, *Science* **264**, 817 (1994).
7. G. H. Olivé and S. Olivé, *Chemistry of the Catalytic Hydrogenation of Carbon Monoxide* (Springer-Verlag, Berlin, 1984).
8. E. W. Abel and B. C. Crosse, *Organometal. Chem. Rev.* **2**, 443 (1967).
9. The iron monosulfide used in this study was dry-synthesized at 600° to 700°C from puratronic-grade starting materials (99.99+% purity, obtained from Alpha Chemicals) using standard methods [e.g., G. Kullerud, in *Research Techniques for High Pressure and High Temperature*, G. C. Ulmer, Ed. (Springer-Verlag, New York, 1971), pp. 289–315]. The resultant polycrystalline aggregate was crushed in the presence of ethanol to a mean grain size of 13.8 μm in an agate mortar while blanketed with argon. The crystal structure of the synthetic FeS was determined by x-ray diffraction to be hexagonal, with $a = b = 5.945$ Å, $c = 11.72$ Å (consistent with the distorted nickel-arsenide structure). Analysis of polished sections of the FeS grains using both reflected light microscopy and electron microprobe analysis revealed no other phases. For further details of the synthesis of FeS, see *Science* Online (www.sciencemag.org/feature/data/1052229.shl).
10. D. A. Palmer, D. J. Weselloski, J. L. Bell, *Eos* **74**, 327 (1993).
11. J. A. Haggerty and J. B. Fisher, *Proc. Ocean Drill. Program* **125**, 387 (1992).
12. The mineral surface area was estimated to be 0.04 m^2/g, according to measurement of the particle size distribution by means of transmitted light microscopy, digital image acquisition, and particle analysis software (NIH Image).
13. The apparatus has been described in detail [e.g., H. S. Yoder Jr., *Trans. Am. Geophys. Union* **31**, 821 (1950)]. The actual pressures ranged from 50.4 to 51.7 MPa, 98.8 to 103.4 MPa, and 204 to 207 MPa. Pressure fluctuations during each run were no more than ±1.2 MPa.
14. The organics were analyzed with GC-MS after derivatization in either methanolic or propanolic solutions containing BF_3 using standard procedures [e.g., *Handbook of Derivatives for Chromatography*, K. Blau and G. S. King, Eds. (Heyden, Bellmawr, NJ, 1977)] and were chromatographically separated using a 14% cyanopropyl, 86% dimethylsilicone microcapillary column.
15. HPLC analysis was performed using a Biorad Aminex HPX-87H column with a 0.03 M sulfuric acid buffer. Analysis of underivatized aqueous extracts with GC-MS was done with a HP FFAP microcapillary column.
16. Raman spectra were obtained using 514-nm Ar^+ laser excitation with about 30 mW laser power. Spectra were acquired with a TRIAX 550 spectrometer equipped with ANDOR Peltier charge-coupled device detector.
17. R. B. King and M. B. Bisnette, *Inorg. Chem.* **4**, 1663 (1965).
18. Analysis of the residual sulfides with an electron microprobe revealed that the FeS composition remained essentially unchanged. The recovered sulfides from three runs at a given pressure corresponded to 69 ± 3.1% (50 MPa), 55.0 ± 19.7% (100 MPa), and 42.4 ± 31.4% (200 MPa), the weight of the initial sulfide charge.
19. R. Hekinanian, M. Chaigneau, J. L. Cheminée, *Nature* **245**, 371 (1973).

20. J. J. Mayerle, S. E. Denmark, B. V. Dephamphilis, J. A. Ibers, R. H. J. Holm, *J. Am. Chem. Soc.* **97**, 1032 (1975).
21. J. W. Peters, W. N. Lanzilotta, B. J. Lemon, L. C. Seefeldt, *Science* **282**, 1853 (1998).
22. M. W. W. Adams and E. I. Stiefel, *Science* **282**, 1842 (1998).
23. Pyruvate was identified by retention time using HPLC and GC-MS (after conversion to both its methyl and propyl derivatives). Pyruvate was not detected in any blank runs. Because of its better chromatographic resolution, GC-MS was used for quantitation of pyruvate yield; the total ion current was calibrated with solutions containing known quantities of derivatized pyruvate.

24. This research was carried out under the auspices of the NASA Astrobiology Institute under NASA Cooperative Agreement NAI NCC2-1056. We thank J. Brandes, M. Fogel, and M. McCarthy for insightful discussions and H. Yang and J. Adler for x-ray diffraction data collection.

16 May 2000; accepted 5 July 2000

Galileo Magnetometer Measurements: A Stronger Case for a Subsurface Ocean at Europa

Margaret G. Kivelson,* Krishan K. Khurana, Christopher T. Russell, Martin Volwerk, Raymond J. Walker, Christophe Zimmer

On 3 January 2000, the Galileo spacecraft passed close to Europa when it was located far south of Jupiter's magnetic equator in a region where the radial component of the magnetospheric magnetic field points inward toward Jupiter. This pass with a previously unexamined orientation of the external forcing field distinguished between an induced and a permanent magnetic dipole moment model of Europa's internal field. The Galileo magnetometer measured changes in the magnetic field predicted if a current-carrying outer shell, such as a planet-scale liquid ocean, is present beneath the icy surface. The evidence that Europa's field varies temporally strengthens the argument that a liquid ocean exists beneath the present-day surface.

Europa, one of the icy moons of Jupiter, may have a layer of liquid water beneath its surface. Features of Europa's tortured surface revealed by Galileo's imaging system may have formed as its surface ice stretched, broke, and rearranged itself while floating on a watery subsurface sea (*1*–*4*). But even if water shaped the surface we see today, it may have frozen hundreds of thousands of years ago. Those searching for possible abodes of life elsewhere in the solar system would like to know whether water exists beneath the surface at the present epoch.

In the initial report (*5*), the magnetic perturbations measured on Galileo's first pass by Europa were characterized as the signature of an internal dipole moment. The Galileo magnetometer team subsequently reported (*6*, *7*) that many features of their data on close passes by Europa in 1996 and 1998 can be modeled as the electromagnetic response to Jupiter's time-varying magnetospheric magnetic field if a layer of electrically conducting material exists near Europa's surface. Although the dominant, southward-oriented magnetic field imposed by Jupiter's magnetosphere at Europa's position is about constant, the projection of the magnetospheric field into Europa's equatorial plane varies with the synodic period (Jupiter's rotation period, 11.2 hours as seen from Europa) and has a mean value close to zero. Such a time-varying magnetic field, referred to as the primary field, can drive inductive currents through an electrical conductor. Inductive currents, in turn, generate a secondary field, whose source can be represented as a time-varying magnetic dipole moment lying in Europa's equatorial plane with an orientation approximately antiparallel to the instantaneous orientation of the primary field (*8*, *9*). If one models Europa as an idealized, highly conducting sphere (conductivity $\gg 1$ S m^{-1}) of radius 1 R_E (radius of Europa = 1560 km) and if the primary field ($B_x(t)$, $B_y(t)$, B_z) is uniform over the scale of Europa, then the components (*10*) of the induced magnetic moment (**M**) are $-1/2(B_x(t), B_y(t),0)$ in magnetic field units, implying that at the surface of Europa, the radial components of the induced field and the time-varying primary field cancel. Table 1 gives values of this idealized induced dipole moment at the time of closest approach (labeled "Ind") and other key parameters of all Europa passes for which the magnetometer acquired data (E4, E11, E12, E14, E15, E17, E19, and E26). We shall focus hereafter only on passes that came within 2000 km of Europa's surface (E4, E12, E14, E19, and E26) for which the signatures of internal sources can have amplitudes large enough to be clearly detected (*11*).

The idealized induction model is consis-

Table 1. Idealized induced dipole moment at closest approach and key parameters of Europa passes. Fitted int, fitted interval; Mag lat and SIII long, System III latitude and longitude; CA, closest approach above Europa's surface; Europa lat and E-long, Europacentric latitude and longitude measured eastward; Bf, best-fit (or measured) dipole model; Ind, induced dipole model.

	E4		E11		E12		E14	
Date	19 December 1996		6 November 1997		16 December 1997		29 March 1998	
Fitted int (UT)	06:32–07:10		20:30–21:00		11:45–12:15		13:05–13:40	
Mag lat (°)	6.5		8.7		−0.8		9.2	
SIII long (°)	157		223		118		184	
CA altitude (km)	688		2039		196		1649	
Europa lat (°)	−1.6		26		−8.6		12	
Europa E-long (°)	322		219		134		131	
	BF	Ind	BF	Ind	BF	Ind	BF	Ind
M_x (nT)	8	−27	−7	21	−61	−39	−16	−5
M_y (nT)	97	88	−25	96	14	16	160	108
M_z (nT)	−52	0	−122	0	392	0	167	0
	E15		E17		E19		E26	
Date	31 May 1998		26 September 1998		1 February 1999		3 January 2000	
Fitted int (UT)	21:12–21:30		03:40–04:20		02:00–02:38		17:45–18:15	
Mag lat (°)	−0.5		3.8		4.8		−9.6	
SIII long (°)	293		138		256		2	
CA altitude (km)	2519		3588		1444		373	
Europa lat (°)	14.9		−42.5		31.0		−46.4	
Europa E-long (°)	225		220		29		83	
	BF	Ind	BF	Ind	BF	Ind	BF	Ind
M_x (nT)	−65	33	152	−38	108	33	−42	11
M_y (nT)	−107	−18	269	47	−12	39	−126	−104
M_z (nT)	−278	0	−496	0	192	0	83	0

Institute of Geophysics and Planetary Physics, University of California, Los Angeles, CA 90095–1567, USA.

*To whom correspondence should be addressed. E-mail: mkivelson@igpp.ucla.edu